# Structure and Chemical Properties of Oxide Nanoparticles Determined by Surface-Ligand IR Spectroscopy

Christof Wöll*

Institute of Functional Interfaces (IFG), Karlsruhe Institute of Technology (KIT), 76344 Eggenstein Leopoldshafen, Germany

ABSTRACT: Recent progress in instrumentation has provided the basis for characterizing the surfaces of catalytically active oxide materials by using surface ligand IR (SLIR) spectroscopy. Reference data have been obtained for molecular ligands, in particular for CO bound to macroscopic, well defined oxide single crystal surfaces, and now allow identifying the facets exposed by nanoparticles. These advances are highly beneficial in the context of in situ and operando studies on catalytically active powder materials, thus allowing the observation of dynamic changes of the shapes of oxide nanoparticles as well as the number, size, type, and charge state of exposed metal particles/clusters. In particular, the SLIR method can also be used to identify single atom active sites in heterogeneous catalysis. Finally, such accurate reference data acquired for well characterized monocrystalline surfaces are required to validate theoretical approaches.

KEYWORDS: oxide surfaces, titania, ceria, IR spectroscopy, nanoparticles, ligands, carbon monoxide
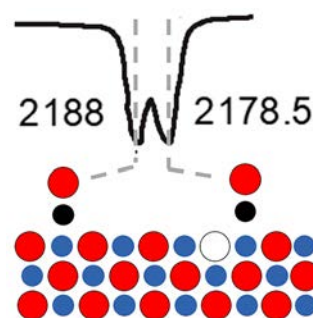
T o achieve a full understanding of chemical processes taking place at the exposed surfaces of oxide nano particles or of metal clusters deposited on oxide nanoparticles will require in situ and operando investigations. The so called surface science approach[1] developed to unravel basic mechanisms of catalytic reactions relies on determining the atomic structure and the behavior of various adsorbates on structurally well defined metal oxide surfaces. Although this approach has been tremendously successful, studies with model systems under idealized, ultrahigh vacuum conditions do not sufficiently describe all processes occurring during the technical process. Researchers have reported cases where dynamic phenomena occur under reaction conditions, which lead to modifications of nanoparticle shape and surface decoration and, in turn, strongly influence a catalyst's performance.[2,3]

Our knowledge of the details of oxide surfaces, including the precise structure of the stoichiometric oxide/vacuum inter faces, as well as a thorough description of typical active sites on oxides such as oxygen vacancies, has advanced in recent years. Comprehensive information on the chemical activity of this important class of materials—with the exception of Au, all metals are coated by a thin oxide layer under ambient conditions—has been gathered by investigating the interaction of oxides with small molecules such as CO, O_2, methanol, and water. Frequently occurring surface species on oxides, e.g. hydroxyl and methoxy groups, have also been investigated. In addition, the mechanisms governing the adhesion of metal atoms and small clusters, as well as the growth mechanism of metal deposits on oxidic substrates, have been identified.

For transition metal oxide substrates, the (110) oriented surface of rutile TiO_2 has provided much of our knowledge.[4] Most of the information on the properties of fully oxidized titania surfaces, with respect to the most important types of defects on this model substrate and their chemical activity, has

come from scanning tunneling microscopy (STM). Often, results from STM have clarified results from other techniques such as thermal desorption spectroscopy (TDS), low energy electron diffraction (LEED), and different variants of photo electron spectroscopy (XPS, UPS). STM can also be applied at higher pressures,[5] but the application of this scanning probe technique to real catalyst powders consisting of crystallites with dimensions in the 100 nm regime is virtually impossible. The difficulties also apply in the case of atomic force microscopy (AFM), which recently has demonstrated atomic resolution on a number of oxide surfaces. The application of photoelectron spectroscopy to powders is hampered not only by charging problems but also by the finite escape depths of the photoelectrons. The latter limits the application of this technique to the uppermost layer of powder particles.

A method well suited for studying powders, under typical reaction conditions, is extended X ray absorption fine structure spectroscopy (EXAFS).[6] However, EXAFS is not strictly surface sensitive, and therefore, it can be unclear if the phenomena observed with this technique are of direct consequence for gas phase species interacting with the surface of the catalyst.

In this context, infrared (IR) spectroscopy plays an important role. This technique can be used to measure vibrational frequencies of molecules weakly bound to surfaces (Figure 1). This method can be applied to single crystal model systems suited for a validation of theoretical approaches, as well as for powders, the technologically relevant form of catalysts, under specific reaction conditions.[7] It is possible to record spectra for catalyst powders under operando conditions
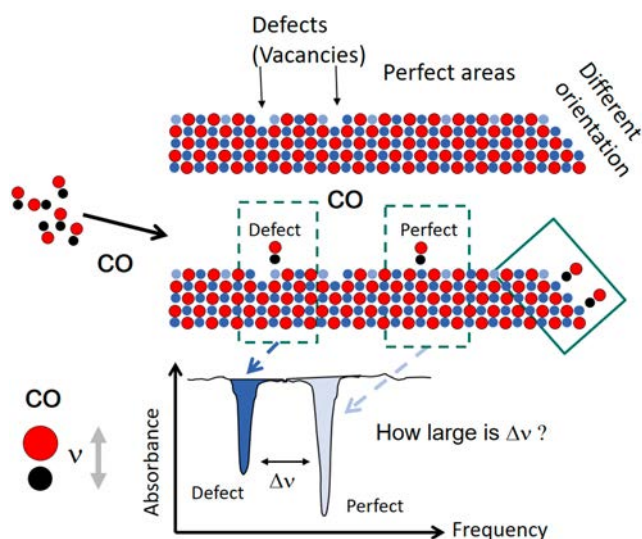
Figure 1. Principle of the CO surface ligand IR approach. The stretching frequency of molecules weakly bound to oxides is extremely sensitive to the environment of the adsorption site.

at pressures up to 50 bar[8] by employing state of the art DRIFTS (diffuse reflectance infrared spectroscopy) techniques. At the same time, reference spectra at the surfaces of macroscopic single crystals and of metal particles deposited on single crystals can be measured.[7] Note that this method has also been applied successfully to characterize single, catalytically active Pt atoms deposited on ceria particles.[9]

For in situ and operando studies of catalytic processes under real conditions, IR spectroscopy offers a number of advantages over other methods. However, in the past IR spectroscopy applied to powder materials has suffered from the drawback that an assignment of the vibrational bands of common small adsorbates bound to the surfaces exposed on the powder particles is not straightforward, since many different surface orientations are present at the same time. In addition, studies of the signatures of imperfections when powdered materials are used represent a major challenge. For example, with CO adsorbates, it is unclear whether the different bands observed on, for example, CeO_2 powders originate from different surface orientations, different charge states of Ce cations, or defects and impurities within the surface.[10]

It should be possible to compute these shifts using theoretical approaches: e.g., density functional theory (DFT). However, the description of oxides and in particular their band gaps with DFT remains a challenge, particularly with simple functionals.[11] In addition, the interaction of weakly bound molecules such as CO often requires the consideration of additional van der Waals terms. Thus, employing theoretical methods to compute vibrational frequencies of weakly bound adsorbates on oxides is far from being straightforward. Rendering predictive power to computational approaches will therefore require validation by experimental studies on well defined model systems: i.e., data recorded under ultrahigh vacuum (UHV) conditions for surfaces of structurally well defined macroscopic single crystal oxides.

Although the potential to use CO as a probe molecule has been realized earlier,[12,13] and in fact this small diatomic has become the most commonly investigated adsorbate on surfaces of oxides, only limited experimental data for well defined macroscopic oxide single crystals have been reported. The first

studies of this type were reported in 1995 by Heidberg and co workers, who were able to record IR data in transmission for single crystal MgO substrates obtained by cleaving.[14] These reference data were then also used to analyzethe corresponding IR results for MgO powder materials[15] and for the validation of theoretical results.[16]

It took until 2008 until the first IR data for CO adsorbed on a monocrystal transition metal oxide became available (rutile $TiO_2(110)$[17]). The delayed application of IR spectroscopy to macroscopic single crystal surfaces of metal oxides by several decades with respect to the characterization of powder materials is due to technical reasons.[18] The main obstacle in this context is the very small reflectivity of dielectrics in the IR region, which turns the recording of IR spectra for single crystal surfaces of oxides in a reflection geometry into a formidable task. In very few cases, electron energy loss spectroscopy, or EELS, could be applied to measure, for example, the stretching frequency of CO,[19] CO_2,[20] and OH adsorbed on macroscopic ZnO single crystals.[21] However, due to the strong intensity of optical phonons (Fuchs−Kliewer modes) during electron scattering, data analysis is difficult and requires a complicated deconvolution process. In addition, the energy resolution of EELS is somewhat limited. Although for metal substrates modern instruments provide resolutions on the order of 1−2 meV, to our knowledge for oxide substrates the best resolution so far amounts to about 6 meV.[21] As a result of this limited resolution in EELS applied to oxides, the observation of small shifts on the order of 1 meV or less, e.g., induced by oxygen vacancies (see below), is extremely challenging. Investigating adsorbate vibrations on oxide powders with EELS is virtually impossible.

A solution to this problem is to study thin oxide films supported on a metal substrate by infrared reflection absorption spectroscopy (IRRAS). In this case, the supporting metal acts as a mirror, thus tremendously increasing intensities. As a result, IR spectra of adsorbates bound to the surfaces of such thin oxide films can be recorded in a straightforward fashion and IR spectroscopy for metal supported oxide thin films is a well developed field.[16] However, because of the lattice mismatch of the oxide on the supporting metal, the fabrication of systems with low defect densities is a challenge. In addition, at least for thin metal oxide films, charge transfer from the metal substrate to the oxide may affect the properties of the latter, complicating a direct comparison to theoretical results obtained for the oxide. Finally, the supporting metal can screen the component of the E vector of the incident IR light parallel to the surface, making it impossible to study adsorbate vibrations parallel to the substrate.

In case of transition metal oxides—which cannot be prepared in a straightforward way by cleaving (as e.g. MgO, see above)—the first IRRAS study for a molecular adsorbate on transition metal oxide single crystal surfaces was published in 1999 by Hayden and co workers.[22] They reported s and p polarized spectra for a formate species bound to a rutile $TiO_2(110)$ surface and were able to determine the molecular orientation as well as the azimuthal alignment from a detailed analysis of the data. Further progress in this field, including the first IRRAS spectra of CO adsorbed to single crystals of this important model substrate,[17] would not come for another 10 years, when data from other groups became available.[23]

Although IR spectroscopy for adsorbates, including CO, bound to oxide powder particles had been in use for a number of years, a reliable identification of the different vibrational

bands was not possible due to the aforementioned lack of appropriate reference data for well defined monocrystal substrates. In fact, a number of early assignments of vibrational bands observed for powder data were not correct. In this context, the vibrational frequency of CO adsorbed to surfaces of (111) oriented surfaces of ceria, $CeO_2(111)$, provides an instructive example. In earlier studies on ceria powders,[25] a band at 2157 cm^{-1} was assigned to physisorbed species and a vibration at 2168 cm^{-1} was attributed to CO bound at Ce^{4+} species. Recent work on the adsorption of CO on surfaces of correspondingly oriented macroscopic single crystal substrates revealed that this assignment must be revised. The two species at 2154 and 2170 cm^{-1} have to be assigned to CO bound to Ce^{4+} within two differently oriented ceria surfaces, $CeO_2(111)$ and $CeO_2(110)$.[26] Different frequencies of adsorbed CO for differently oriented metal oxide single crystals have also been observed for other materials: e.g., in the case of $ZnO(10\bar{1}0)$ and $ZnO(11\bar{2}0)$ the stretching frequencies at full coverage are found at 2169 and 2181 cm^{-1}, respectively.[27]

In addition to CO bound to ceria, other examples have demonstrated that the reliable assignment of adsorbate vibrational frequencies observed for powder particles is only possible when data for single crystal reference systems have been determined.

The availability of such validated assignments in recent years,[7] as well as vibrational spectroscopy of simple ligands, particularly CO, bound to oxide surfaces has allowed a substantial advance in the approach to characterize powder particles. Investigating the vibrational spectra of probe molecules bound to oxides of unknown shape provides information on the oxide surfaces exposed. In fact, using vibrational frequencies of adsorbed probe molecules, which in the context of this perspective we will refer to as CO SLIR (surface ligand IR spectroscopy), permitted observation of some surprising phenomena. An instructive example is the evolution of the shape of oxide nanoparticles upon heating and under reaction conditions.

For ceria, the different shapes of nanoparticles result in strongly different catalytic activities.[24,28] Ceria nanorods can be prepared using appropriate synthesis conditions. Transmission electron microscopy (TEM) reveals that they are mainly terminated by (110) surfaces, with small portions of (100) facets exposed at the top and at the bottom (Figure 2)

After exposure of these nanoparticles to CO at temperatures of approximately 60 K, the typical frequency of CO bound to $CeO_2(110)$, 2170 cm^{-1}, is first observed in the IR data (Figure
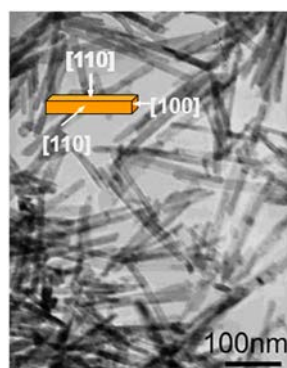
Figure 2. Images of CeO_2 nanorods. The TEM micrographs are from ref 24. Adapted with permission from ref 24. Copyright 2005, Elsevier.

3),[26] fully consistent with the rod shaped form of the particles as seen in the TEM data. However, a distinct second peak at
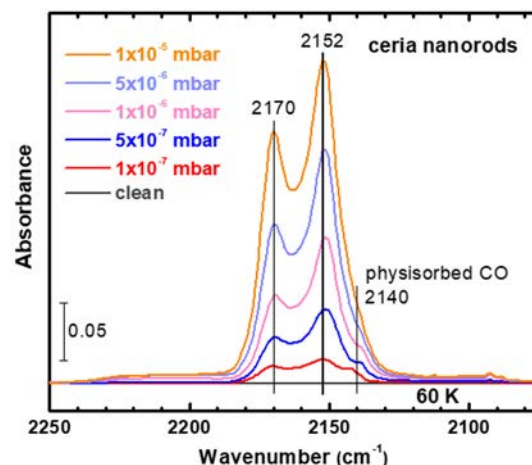
Figure 3. IR data for CO adsorbed on ceria nanorods recorded at 60 K. Data from ref 26.

2152 cm^{-1} is present, which was not seen for the reference (110) surface. Also for the (100) surface (the ends of the nanorods are capped by facets with this orientation) a different frequency, 2176 cm^{-1}, was observed. A straightforward assignment of the 2152 cm^{-1} peak is to {111} terminated facets. The presence of such differently oriented surface areas is incompatible with the ideal shape of ceria nanorods, as seen in the TEM data (Figure 2).

To resolve this apparent inconsistency, a thorough surface science study was carried out for the reference system, macroscopic (110) substrates. For the fully oxidized substrate, only one sharp band at 2170 cm^{-1} was seen. Indeed, after harsh preparation conditions, including prolonged sputtering and annealing the (110) substrates to temperatures above 527 °C, a new vibrational band was observed, with the same frequency as for the nanorods, 2152 cm^{-1}. At the same time, LEED data recorded for the surface showed a pronounced restructuring. Furthermore, the presence of only one negative absorbance band at 2152 cm^{-1} in the s polarized IR data led to the conclusion that facets with pronounced tilt angles relative to the surface must be present. Since the new vibrational frequency observed after heating is that typical for CO adsorbed on (111) terminated CeO_2 substrates, it was straightforward to speculate that upon heating a nanofaceting takes place, leading to the presence of areas with (111) surface termination. These observations can be rationalized by considering the thermodynamics of ceria—the (111) surface is much more stable than (110) or (100).[29] Indeed, an intense effort using a high resolution TEM confirmed this hypothesis and demonstrated the presence of sawtoothlike {111} nanofacets for the ceria nanorods, with facet sizes on the order of 20 nm.[26]

This example demonstrates that the CO SLIR approach carries great potential for characterization of the surfaces of metal oxide nanoparticles under realistic conditions. A reliable interpretation of the IR spectra recorded for small molecules bound to powder samples requires reference data recorded for macroscopic single crystal substrates. It is worth noting that only such structurally well characterized samples provide a reliable validation of theoretical results. Of course, a full

structural characterization of an oxide single crystal surface is not possible by IR spectroscopy alone. Here other techniques such as surface X ray diffraction, scanning tunneling micros copy, and photoelectron spectroscopy are required. However, in many systems the preparation of well defined single crystal surfaces has been reported in the literature, so that when the corresponding IRRAS data are recorded, one can rely on previously established preparation procedures.

Certainly, for a complete description of chemical reactions occurring at the surfaces of oxides, a consideration of only fully oxidized substrates is insufficient. In many cases, chemical activity is intimately related to the presence of active sites, with oxygen vacancies representing the most important type. Metal oxides are often used as oxidation catalysts: e.g., in the context of reducing volatile organic compounds (VOC) in the exhaust gas of combustion engines to fulfill the requirements of air pollution control regulations.[30] For ethanol, the O atoms required for partial oxidation are abstracted from the catalyst and are replenished from the gas phase by dissociation of O_2 (Mars−van Krevelen mechanism).

Therefore, monitoring the density of O vacancies is essential in characterizing the reaction mechanism. The determination of O vacancies and the characterization of catalytic activity on macroscopic single crystal substrates is possible with STM, although on several occasions a reliable distinction of O vacancies and adsorbed hydroxyl groups has been found to be difficult: e.g., on rutile $TiO_2(110)$.[32] Furthermore, the application of the STM technique to powder particles is virtually impossible. Thus, for identification of the role of O vacancies under catalytic conditions, the CO SLIR approach provides an important alternative.

In this context, the application of CO SLIR requires a knowledge of the shift in frequency induced by imperfections such as O vacancies. In the past, we had an incomplete understanding of how large the defect induced shifts in CO vibrational frequency were. Once these shifts were determined on the surfaces of macroscopic rutile $TiO_2(110)$ surfaces with defects prepared by procedures established in detailed STM investigations, the application to titania powders became possible. As demonstrated by the IRRAS data shown in Figure 4, these shifts were found to be unexpectedly small (10 cm^{-1}).[31] Indeed, CO probe molecules allowed the successful detection of O vacancies also on r TiO2 powder particles (see
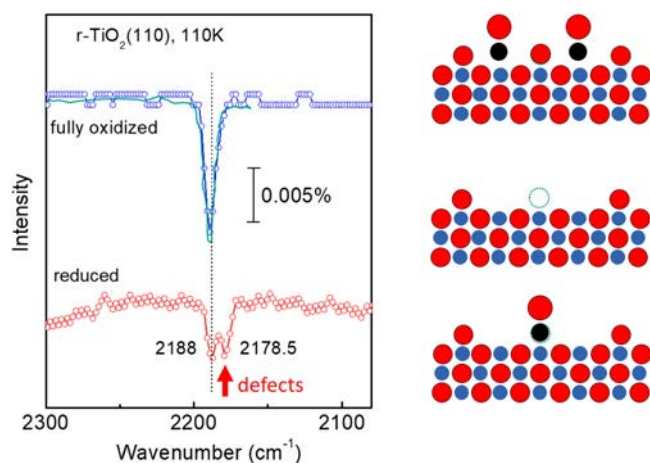

Figure 4. IRRAS data for CO adsorbed on a fully oxidized and a reduced r $TiO_2(110)$ substrate. Data from ref 31.

Figure 5) and demonstrated that, in a prototypical C−C coupling reaction, the dimerization of formaldehyde to yield diolate species is only possible in the presence of O vacancies.[31,33]
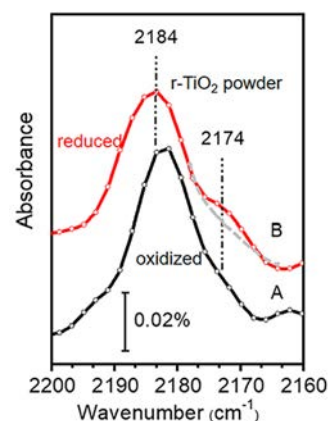

Figure 5. IRRAS data for CO adsorbed on fully oxidized and reduced r TiO_2 powder. Data from ref 31.

In a few cases, the thermodynamically most favorable location of O vacancies is not at the surface of the oxide but, rather, deeper in the surface. The most prominent example is anatase $TiO_2(101)$, where experimental STM data and theoretical findings clearly demonstrated that vacancies migrate to deeper layers after they are created at the surface.[34] In related investigations, the CO SLIR method provided an independent confirmation of this finding.[35]

For anatase $TiO_2(101)$, the subsurface O vacancies have only a small effect on the CO vibrational frequency.[35] In contrast, for the $CeO_2(111)$ surface, the O vacancies are proposed to be located in the second layer, yielding a shift of the CO stretching frequency of 8 cm^{-1}.[36] Notably, in this case the reduction of the oxide substrate causes a blue shift, while on $TiO_2(110)$ a red shift was seen.[31]

Interestingly, the behaviors for the $CeO_2(100)$ and $CeO_2(110)$ surfaces are different. In these cases, dioxygen adsorption experiments on reduced surfaces of the correspond ing single crystals revealed the formation of peroxo (O_2^{2-}) and superoxo (O_2^-) species.[36] Although the excitation of the O_2 stretching vibration is symmetry forbidden in the gas phase, the negatively charged molecules bound to a substrate can be observed in IRRAS. The assignment of the vibrational bands is straightforward, since the corresponding frequencies are known from Raman spectroscopy.[37] On reduced $CeO_2(111)$ surfaces, however, no such activated O_2 molecules could be observed.[36] This observation is consistent with the O vacancies being located in deeper layers for the (111) surface, but not for the ceria (110) and (100) surfaces, as discussed above.[38]

In recent applications of CO SLIR to a $Fe_2O_3(0001)$ substrate,[39] the observation of one single, sharp band strongly suggested that the fully oxidized surface is terminated by a single type of Fe ion. After a subsequent mild reduction of the surface induced by annealing at elevated temperatures, new vibrational bands were observed, indicating the formation of surface oxygen vacancies. In a second step, the surface was reduced more aggressively by exposure to atomic hydrogen, followed by Ar^+ sputtering and annealing under oxygen poor conditions. As a result of this reduction, a massive rearrange ment was observed at the iron oxide/vacuum interface.

Interestingly, CO adsorbed on this rearranged surface showed positions of its vibrational band characteristic for CO bound to $Fe_3O_4(111)$.[39] This result led to the conclusion that a $Fe_3O_4(111)/Fe_{1-x}O(111)$ biphase was formed, with both Fe^{3+} and Fe^{2+} ions exposed at the surface. A comparison to data for fully oxidized $Fe_3O_4(111)$ indicated that this biphase consisted of patches with perfect Fe_{oct2} termination, coexisting with areas showing a $Fe_{1-x}O(111)$ termination containing $Fe^{2+}(oct)$ species.[39]

CO SLIR investigations have also been applied to structural changes in oxide thin layers induced by charge transfer from the substrate. Thin layers of ZnO deposited on noble metal substrates provide an instructive example. Earlier theoretical work[40] had shown that in thin films (up to about 10 layers), ZnO adopts a layered structure, distinct from the wurtzite arrangement present in the bulk. For thin films of ZnO grown on Cu(111), application of the CO SLIR approach revealed a CO stretching frequency of 2116 cm^{-1}.[41] The observation of such a red shifted (relative to the gas phase) frequency is quite unusual; normally CO bound to metal oxides shows a blue shift. Theoretical work using DFT revealed that for the layered form of ZnO such a blue shift is expected.[41] Indeed, the frequency of 2116 cm^{-1} is quite far away from the CO stretching frequencies observed for any single crystal ZnO surfaces, which are all shifted to higher frequencies. More detailed theoretical investigations revealed that these thin ZnO layers grown on Cu(111) are affected by a small charge transfer from the metallic substrate.[41] As a result, there is an additional charge in the oxide thin film, which in turn changes the bonding of CO and, correspondingly, the stretching frequency of this probe molecule. A similar behavior was observed for ZnO/Ag(111)[42] and has also been predicted to occur for thin ZnO layers deposited on Au(111).[43]

The occurrence of such ZnO thin films covering the Cu particles used in methanol synthesis was proposed on the basis of indirect evidence.[44] Interestingly, the presence of this layered form of ZnO encapsulating Cu particles in a real catalyst could be shown directly in high resolution TEM,[45] and DRIFTS experiments revealed that the same frequency as seen in the model system experiments was also observed for CO adsorbed on the active catalyst.[46]

The applicability of the SLIR approach is not limited to stoichiometric and reduced oxides but can also be used to determine the chemical properties of deposited metal atoms and clusters. Of particular interest in this context is that the CO stretching frequency is sensitive not only to the type of metal but also to its charge state. In the case of isolated Cu ions, for example, the difference in frequency between CO/Cu^+ and CO/Cu^{2+} amounted to about 40 cm^{-1},[48] a fairly large value.

Recently, a multitechnique investigation of ultrafine Cu clusters supported on ceria nanorods underscored the ability of CO SLIR to identify differently charged metal ions.[47] First, high resolution TEM allowed determination of the morphology of the Cu islands, with most of them adopting a bilayer structure (Figure 6). Then, CO SLIR investigations (Figure 7) demonstrated that the metal bilayers consisted mainly of uncharged Cu^0 species at the top layer, but with a rim of Cu^+ ions at the metal/substrate interface, as illustrated in Figure 6. Systematic experiments for Cu/CeO$_2$ catalysts activated in hydrogen at different temperatures revealed a clear correlation of the total rim lengths with the catalytic performance. Theses experimental observations, together with the IR data obtained
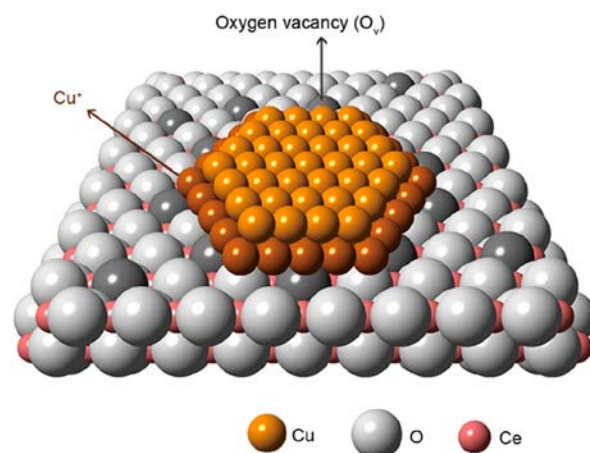

Figure 6. Cu islands deposited on ceria nanocubes. Reproduced with permission from ref 47. Copyright 2019, Nature Publishing Group.

for CO/D$_2$O coadsorption and a theoretical analysis using DFT, then allowed the determination of the active sites for the water gas shift reaction.[47]

The CO SLIR approach was also applied to Au deposited on ZnO powder particles.[49] For deposits of this noble metal, which reveal a surprisingly high catalytic activity, a number of different Au induced bands were clearly observed, including one at 2106 cm^{-1} assigned to neutral Au, and bands at 2077 cm^{-1} related to an Au$^{\delta-}$ band and one at 2138 cm^{-1} related to Au$^{\delta+}$. The observation of these different vibrations was used to propose a mechanism for the low temperature CO oxidation observed on these catalytically very active powder samples.

In fact, the CO SLIR approach can also be applied to bimetallic deposits on oxides. In a recent study,[50] AuPd clusters, which show significantly higher chemical activity and selectivity in comparison to their single metal counterparts, were deposited on TiO$_2$ powder particles and then subjected to a multitechnique investigation. Using the CO SLIR approach, the different metal ions present at the surface of the metal decorated oxide nanoparticles (Ti^{4+}, Pd^{2+}, Au^0, atop Pd^0, and bridge Pd^0) could be clearly distinguished from the different positions of the CO vibrational bands.

The recent progress in experimental IRRAS instrumentation has led to the creation of a library containing many experimental frequencies of CO ligands bound to numerous different oxide surfaces, including CeO$_2$, rutile TiO$_2$, anatase TiO$_2$, Fe$_2$O$_3$, Fe$_3$O$_4$, and ZnO. These experimental results are provided in Table 1. In many cases, theoretical results, mostly from DFT, have also become available, putting the assignment of the vibrational bands on a solid theoretical basis and—very importantly—allowing the acquisition of at least semi quantitative information on the assignment of the vibrational bands. We foresee that, with this experimental information at hand, future interpretations of CO SLIR spectra will develop into a routine technique for catalyst characterization. In this context, it is important to note that the SLIR technique is not restricted to UHV conditions. Polarization modulation IR spectroscopy can be used to extend studies of macroscopic single crystal surfaces to conditions of ambient pressures.[13] With regard to the technical process, it is important to point out that DRIFTS studies for powder samples can be extended to ambient pressure and above (experiments at 50 bar have been reported[8]). We wish to point out that O$_2$ SLIR may gain
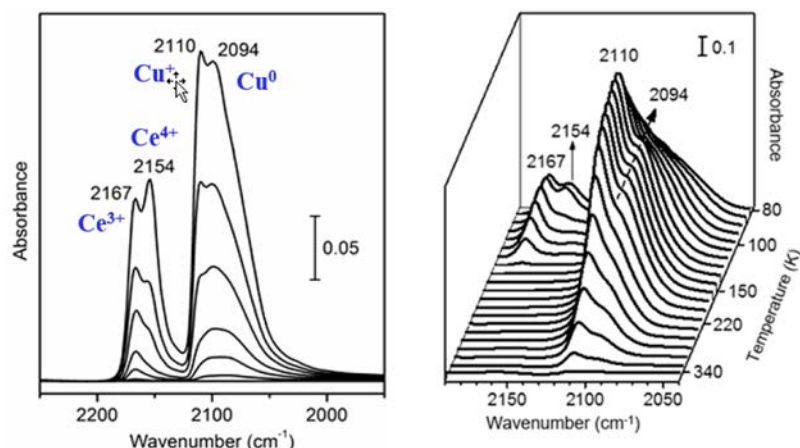
Figure 7. IR data for CO adsorbed on Cu/ceria nanorods. Bands for CO adsorbed on the oxidic substrate can be clearly distinguished from CO species bound to Cu sites. Reproduced with permission from ref 47. Copyright 2019, Nature Publishing Group.

Table 1. IRRAS Works on Transition Metal Oxide Single Crystals

oxide	orientation	adsorbate	ref
ZnO	(10 10)	CO	27
		CO_2	51, 52
		H_2O	53
		HCOOH	54
	(11 20)	CO	27
TiO$_2$ rutile	(110)	CO	55 61
		CO_2	62, 63
		NO	55, 64 66
		CH_3OH	67
		CH_2O	33
		HCOOH	22, 68, 69
		O_2; HCOOH	70
		H_2O	71, 72
		acetone	73, 74
		benzoic acid	75
		terephthalic acid	75
		benzaldehyde	76
TiO$_2$ anatase	(101)	CO	77
		CO_2	51
		HCOOH	55, 78
Fe$_2$O$_3$	(0001)	CO	79
		H_2O	80
Fe$_3$O$_4$	(111)	CO	39
	(001)	CO	39
		HCOOH	81
CeO$_2$	(111)	CO	10
		O_2	18
		N_2O	26
		CH_3OH	82
	(110)	CO	26
		O_2	18
		N_2O	83
		CH_3OH	82
	(100)	O_2	18

more importance in the future, since the O_2 vibration is silent in the gas phase but can be detected for adsorbed dioxygen species.[36] As a result, in operando experiments at high pressures become possible, since the gas phase signal obscuring the signal from the O_2 adsorbates is absent.

We also see the prospect of time resolved studies. In this case, switching between different isotopes provides a way to gain direct insights into catalytic investigations.

AUTHOR INFORMATION

Corresponding Author

*E mail for C.W.: christof.woell@kit.edu.

ORCID ◉

Christof Wöll: 0000 0003 1078 3304

Notes

The author declares no competing financial interest.

REFERENCES

(1) Ertl, G.; Freund, H. J. Catalysis and surface science. *Phys. Today* **1999**, *52*, 32−38.

(2) Newton, M. A. Dynamic adsorbate/reaction induced structural change of supported metal nanoparticles: heterogeneous catalysis and beyond. *Chem. Soc. Rev.* **2008**, *37*, 2644−2657.

(3) Schauermann, S.; Nilius, N.; Shaikhutdinov, S.; Freund, H. J. Nanoparticles for Heterogeneous Catalysis: New Mechanistic In sights. *Acc. Chem. Res.* **2013**, *46*, 1673−1681.

(4) Diebold, U. The surface science of titanium dioxide. *Surf. Sci. Rep.* **2003**, *48*, 53−229.

(5) Hendriksen, B. L. M.; Frenken, J. W. M. CO oxidation on Pt(110): Scanning tunneling microscopy inside a high pressure flow reactor. *Phys. Rev. Lett.* **2002**, *89*, 046401.

(6) Kalz, K. F.; Kraehnert, R.; Dvoyashkin, M.; Dittmeyer, R.; Glaser, R.; Krewer, U.; Reuter, K.; Grunwaldt, J. D. Future Challenges in Heterogeneous Catalysis: Understanding Catalysts under Dynamic Reaction Conditions. *ChemCatChem* **2017**, *9*, 17−29.

(7) Wang, Y.; Wöll, C. IR spectroscopic investigations of chemical and photochemical reactions on metal oxides: bridging the materials gap. *Chem. Soc. Rev.* **2017**, *46*, 1875−1932.

(8) Abdel Mageed, A. M.; Klyushin, A.; Rezvani, A.; Knop Gericke, A.; Schlogl, R.; Behm, J. Negative Charging of Au Nanoparticles during Methanol Synthesis from CO2/H 2 on a Au/ZnO Catalyst: Insights from Operando IR and Near Ambient Pressure XPS and XAS Measurements. *Angew. Chem., Int. Ed.* **2019**, *58*, 10325−10329.

(9) Jones, J.; Xiong, H. F.; Delariva, A. T.; Peterson, E. J.; Pham, H.; Challa, S. R.; Qi, G. S.; Oh, S.; Wiebenga, M. H.; Hernandez, X. I. P.; Wang, Y.; Datye, A. K. Thermally stable single atom platinum on ceria catalysts via atom trapping. *Science* **2016**, *353*, 150−154.

(10) Yang, C.; Yin, L. L.; Bebensee, F.; Buchholz, M.; Sezen, H.; Heissler, S.; Chen, J.; Nefedov, A.; Idriss, H.; Gong, X. Q.; Wöll, C. Chemical activity of oxygen vacancies on ceria: a combined experimental and theoretical study on CeO2(111). *Phys. Chem. Chem. Phys.* **2014**, *16*, 24165−24168.

(11) Pacchioni, G. First Principles Calculations on Oxide Based Heterogeneous Catalysts and Photocatalysts: Problems and Advances. *Catal. Lett.* **2015**, *145*, 80−94.

(12) Lamberti, C.; Zecchina, A.; Groppo, E.; Bordiga, S. Probing the surfaces of heterogeneous catalysts by in situ IR spectroscopy. *Chem. Soc. Rev.* **2010**, *39*, 4951−5001.

(13) Zaera, F. New advances in the use of infrared absorption spectroscopy for the characterization of heterogeneous catalytic reactions. *Chem. Soc. Rev.* **2014**, *43*, 7624−7663.

(14) Heidberg, J.; Kandel, M.; Meine, D.; Wildt, U. THE MONOLAYER CO ADSORBED ON MGO(100) DETECTED BY POLARIZATION INFRARED SPECTROSCOPY. *Surf. Sci.* **1995**, *331*, 1467−1472.

(15) Spoto, G.; Gribov, E. N.; Ricchiardi, G.; Damin, A.; Scarano, D.; Bordiga, S.; Lamberti, C.; Zecchina, A. Carbon monoxide MgO from dispersed solids to single crystals: a review and new advances. *Prog. Surf. Sci.* **2004**, *76*, 71−146.

(16) Freund, H. J.; Pacchioni, G. Oxide ultra thin films on metals: new materials for the design of supported metal catalysts. *Chem. Soc. Rev.* **2008**, *37*, 2224−2242.

(17) Rohmann, C.; Wang, Y. M.; Muhler, M.; Metson, J.; Idriss, H.; Wöll, C. Direct monitoring of photo induced reactions on well defined metal oxide surfaces using vibrational spectroscopy. *Chem. Phys. Lett.* **2008**, *460*, 10−12.

(18) Yang, C.; Wöll, C. IR spectroscopy applied to metal oxide surfaces: adsorbate vibrations and beyond. *Advances in Physics: X* **2017**, *2*, 373−408.

(19) D'Amico, K. L.; McFeely, F. R.; Solomon, E. I. HIGH RESOLUTION ELECTRON ENERGY LOSS VIBRATIONAL STUDIES OF CO COORDINATION TO THE (1010) SURFACE OF ZNO. *J. Am. Chem. Soc.* **1983**, *105*, 6380−6383.

(20) Wang, Y.; Kovacik, R.; Meyer, B.; Kotsis, K.; Stodt, D.; Staemmler, V.; Qiu, H.; Traeger, F.; Langenberg, D.; Muhler, M.; Wöll, C. CO2 activation by ZnO through the formation of an unusual tridentate surface carbonate. *Angew. Chem., Int. Ed.* **2007**, *46*, 5624−5627.

(21) Wang, Y.; Meyer, B.; Yin, X.; Kunat, M.; Langenberg, D.; Traeger, F.; Birkner, A.; Wöll, C. Hydrogen induced metallicity on the ZnO(10(1)over bar0) surface. *Phys. Rev. Lett.* **2005**, *95*, 266104.

(22) Hayden, B. E.; King, A.; Newton, M. A. Fourier transform reflection absorption IR spectroscopy study of formate adsorption on TiO2(110). *J. Phys. Chem. B* **1999**, *103*, 203−208.

(23) Petrik, N. G.; Kimmel, G. A. Adsorption Geometry of CO versus Coverage on TiO2(110) from s and p Polarized Infrared Spectroscopy. *J. Phys. Chem. Lett.* **2012**, *3*, 3425−3430.

(24) Zhou, K. B.; Wang, X.; Sun, X. M.; Peng, Q.; Li, Y. D. Enhanced catalytic activity of ceria nanorods from well defined reactive crystal planes. *J. Catal.* **2005**, *229*, 206−212.

(25) Binet, C.; Daturi, M.; Lavalley, J. C. IR study of polycrystalline ceria properties in oxidised and reduced states. *Catal. Today* **1999**, *50*, 207−225.

(26) Yang, C.; Yu, X.; Heißler, S.; Nefedov, A.; Colussi, S.; Llorca, J.; Trovarelli, A.; Wang, Y.; Wöll, C. Surface Faceting and Reconstruction of Ceria Nanoparticles. *Angew. Chem., Int. Ed.* **2017**, *56*, 375−379.

(27) Buchholz, M.; Yu, X.; Yang, C.; Heißler, S.; Nefedov, A.; Wang, Y.; Wöll, C. IR spectroscopy of CO adsorption on mixed terminated ZnO surfaces. *Surf. Sci.* **2016**, *652*, 247−252.

(28) Trovarelli, A.; Llorca, J. Ceria Catalysts at Nanoscale: How Do Crystal Shapes Shape Catalysis? *ACS Catal.* **2017**, *7*, 4716−4735.

(29) Paier, J.; Penschke, C.; Sauer, J. Oxygen Defects and Surface Chemistry of Ceria: Quantum Chemical Studies Compared to Experiment. *Chem. Rev.* **2013**, *113*, 3949−3985.

(30) Chuang, K. T.; Zhou, B.; Tong, S. M. KINETICS AND MECHANISM OF CATALYTIC OXIDATION OF FORMALDE HYDE OVER HYDROPHOBIC CATALYSTS. *Ind. Eng. Chem. Res.* **1994**, *33*, 1680−1686.

(31) Xu, M.; Noei, H.; Fink, K.; Muhler, M.; Wang, Y.; Wöll, C. The Surface Science Approach for Understanding Reactions on Oxide Powders: The Importance of IR Spectroscopy. *Angew. Chem., Int. Ed.* **2012**, *51*, 4731−4734.

(32) Wendt, S.; Schaub, R.; Matthiesen, J.; Vestergaard, E. K.; Wahlstrom, E.; Rasmussen, M. D.; Thostrup, P.; Molina, L. M.; Laegsgaard, E.; Stensgaard, I.; Hammer, B.; Besenbacher, F. Oxygen vacancies on TiO2(110) and their interaction with H2O and O 2: A combined high resolution STM and DFT study. *Surf. Sci.* **2005**, *598*, 226−245.

(33) Yu, X.; Zhang, Z.; Yang, C.; Bebensee, F.; Heissler, S.; Nefedov, A.; Tang, M.; Ge, Q.; Chen, L.; Kay, B. D.; Dohnálek, Z.; Wang, Y.; Wöll, C. Interaction of Formaldehyde with the Rutile TiO2(110) Surface: A Combined Experimental and Theoretical Study. *J. Phys. Chem. C* **2016**, *120*, 12626−12636.

(34) He, Y. B.; Dulub, O.; Cheng, H. Z.; Selloni, A.; Diebold, U. Evidence for the Predominance of Subsurface Defects on Reduced Anatase TiO2(101). *Phys. Rev. Lett.* **2009**, *102*, 106105.

(35) Setvin, M.; Buchholz, M.; Hou, W. Y.; Zhang, C.; Stoger, B.; Hulva, J.; Simschitz, T.; Shi, X.; Pavelec, J.; Parkinson, G. S.; Xu, M. C.; Wang, Y. M.; Schmid, M.; Wöll, C.; Selloni, A.; Diebold, U. A Multitechnique Study of CO Adsorption on the TiO2 Anatase (101) Surface. *J. Phys. Chem. C* **2015**, *119*, 21044−21052.

(36) Yang, C. W.; Yu, X.; Heißler, S.; Weidler, P. G.; Nefedov, A.; Wang, Y.; Wöll, C.; Kropp, T.; Paier, J.; Sauer, J. O2 Activation on Ceria Catalysts The Importance of Substrate Crystallographic Orientation. *Angew. Chem., Int. Ed.* **2017**, *56*, 16399−16404.

(37) Wu, Z. L.; Li, M. J.; Howe, J.; Meyer, H. M.; Overbury, S. H. Probing Defect Sites on CeO2 Nanocrystals with Well Defined Surface Planes by Raman Spectroscopy and O 2 Adsorption. *Langmuir* **2010**, *26*, 16595−16606.

(38) Ganduglia Pirovano, M. V.; Da Silva, J. L. F.; Sauer, J. Density Functional Calculations of the Structure of Near Surface Oxygen Vacancies and Electron Localization on CeO2(111). *Phys. Rev. Lett.* **2009**, *102*, 026101.

(39) Schottner, L.; Nefedov, A.; Yang, C. W.; Heissler, S.; Wang, Y. M.; Wöll, C. Structural Evolution of alpha Fe2O3(0001) Surfaces Under Reduction Conditions Monitored by Infrared Spectroscopy. *Frontiers in Chemistry* **2019**, *7*, 12.

(40) Freeman, C. L.; Claeyssens, F.; Allan, N. L.; Harding, J. H. Graphitic nanofilms as precursors to wurtzite films: Theory. *Phys. Rev. Lett.* **2006**, *96*, 066102.

(41) Schott, V.; Oberhofer, H.; Birkner, A.; Xu, M. C.; Wang, Y. M.; Muhler, M.; Reuter, K.; Wöll, C. Chemical Activity of Thin Oxide Layers: Strong Interactions with the Support Yield a New Thin Film Phase of ZnO. *Angew. Chem., Int. Ed.* **2013**, *52*, 11925−11929.

(42) Andersen, M.; Yu, X. J.; Kick, M.; Wang, Y. M.; Wöll, C.; Reuter, K. Infrared Reflection Absorption Spectroscopy and Density Functional Theory Investigations of Ultrathin ZnO Films Formed on Ag(111). *J. Phys. Chem. C* **2018**, *122*, 4963−4971.

(43) Tosoni, S.; Li, C.; Schlexer, P.; Pacchioni, G. CO Adsorption on Graphite like ZnO Bilayers Supported on Cu(111), Ag(111), and Au(111) Surfaces. *J. Phys. Chem. C* **2017**, *121*, 27453−27461.

(44) Naumann d'Alnoncourt, R.; Xia, X.; Strunk, J.; Loffler, E.; Hinrichsen, O.; Muhler, M. The influence of strongly reducing conditions on strong metal support interactions in Cu/ZnO catalysts

used for methanol synthesis. *Phys. Chem. Chem. Phys.* **2006**, *8*, 1525–1538.

(45) Lunkenbein, T.; Schumann, J.; Behrens, M.; Schlogl, R.; Willinger, M. G. Formation of a ZnO Overlayer in Industrial Cu/ZnO/Al2O3 Catalysts Induced by Strong Metal Support Interactions. *Angew. Chem., Int. Ed.* **2015**, *54*, 4544–4548.

(46) Schumann, J.; Krohnert, J.; Frei, E.; Schlogl, R.; Trunschke, A. IR Spectroscopic Study on the Interface of Cu Based Methanol Synthesis Catalysts: Evidence for the Formation of a ZnO Overlayer. *Top. Catal.* **2017**, *60*, 1735–1743.

(47) Chen, A. L.; Yu, X. J.; Zhou, Y.; Miao, S.; Li, Y.; Kuld, S.; Sehested, J.; Liu, J. Y.; Aoki, T.; Hong, S.; Camellone, M. F.; Fabris, S.; Ning, J.; Jin, C. C.; Yang, C. W.; Nefedov, A.; Wöll, C.; Wang, Y. M.; Shen, W. J. Structure of the catalytically active copper ceria interfacial perimeter. *Nat. Catal.* **2019**, *2*, 334–341.

(48) St. Petkov, P.; Vayssilov, G. N.; Liu, J.; Shekhah, O.; Wang, Y.; Wöll, C.; Heine, T. Defects in MOFs: A Thorough Characterization. *ChemPhysChem* **2012**, *13*, 2025–2029.

(49) Noei, H.; Birkner, A.; Merz, K.; Muhler, M.; Wang, Y. M. Probing the Mechanism of Low Temperature CO Oxidation on Au/ZnO Catalysts by Vibrational Spectroscopy. *J. Phys. Chem. C* **2012**, *116*, 11181–11188.

(50) Tofighi, G.; Yu, X. J.; Lichtenberg, H.; Doronkin, D. E.; Wang, W.; Wöll, C.; Wang, Y. M.; Grunwaldt, J. D. Chemical Nature of Microfluidically Synthesized AuPd Nanoalloys Supported on TiO2. *ACS Catal.* **2019**, *9*, 5462–5473.

(51) Cao, Y.; Yu, M.; Qi, S.; Wang, T.; Huang, S.; Ren, Z.; Yan, S.; Hu, S.; Xu, M. CO2 adsorption on anatase TiO2(101) surfaces: A combination of UHV FTIRS and first principles studies. *Phys. Chem. Chem. Phys.* **2017**, *19*, 31267–31273.

(52) Buchholz, M.; Weidler, P. G.; Bebensee, F.; Nefedov, A.; Wöll, C. Carbon dioxide adsorption on a ZnO(10−10) substrate studied by infrared reflection absorption spectroscopy. *Phys. Chem. Chem. Phys.* **2014**, *16*, 1672–1678.

(53) Yu, X.; Schwarz, P.; Nefedov, A.; Meyer, B.; Wang, Y.; Wöll, C. Structural evolution of water on zinc oxides: From isolated monomers via anisotropic H bonded 2D and 3D structures to isotropic multilayers. *Angew. Chem.* **2019**.

(54) Buchholz, M.; Li, Q.; Noei, H.; Nefedov, A.; Wang, Y.; Muhler, M.; Fink, K.; Wöll, C. The Interaction of Formic Acid with Zinc Oxide: A Combined Experimental and Theoretical Study on Single Crystal and Powder Samples. *Top. Catal.* **2015**, *58*, 174–183.

(55) Noei, H.; Jin, L.; Qiu, H.; Xu, M.; Gao, Y.; Zhao, J.; Kauer, M.; Wöll, C.; Muhler, M.; Wang, Y. Vibrational spectroscopic studies on pure and metal covered metal oxide surfaces. *Phys. Status Solidi B* **2013**, *250*, 1204–1221.

(56) Wang, Y.; Glenz, A.; Muhler, M.; Wöll, C. A new dual purpose ultrahigh vacuum infrared spectroscopy apparatus optimized for grazing incidence reflection as well as for transmission geometries. *Rev. Sci. Instrum.* **2009**, *80*, 113108.

(57) Wang, Y.; Wöll, C. Chemical reactions on metal oxide surfaces investigated by vibrational spectroscopy. *Surf. Sci.* **2009**, *603*, 1589–1599.

(58) Rohmann, C.; Wang, Y.; Muhler, M.; Metson, J.; Idriss, H.; Wöll, C. Direct monitoring of photo induced reactions on well defined metal oxide surfaces using vibrational spectroscopy. *Chem. Phys. Lett.* **2008**, *460*, 10.

(59) Petrik, N. G.; Kimmel, G. A. Adsorption Geometry of CO versus Coverage on TiO2(110) from s and p Polarized Infrared Spectroscopy. *J. Phys. Chem. Lett.* **2012**, *3*, 3425–3430.

(60) Xu, M.; Cao, Y.; Xu, R.; Hu, S.; Yan, S. UHV FTIRS studies on molecular competitive adsorption: 12CO, 13CO and CO2 on reduced TiO2(110) surfaces. *Phys. Chem. Chem. Phys.* **2014**, *16*, 23711–23715.

(61) Hu, S.; Wang, Z.; Mattsson, A.; Österlund, L.; Hermansson, K. Simulation of IRRAS Spectra for Molecules on Oxide Surfaces: CO on TiO2(110). *J. Phys. Chem. C* **2015**, *119*, 5403–5411.

(62) Lin, X.; Yoon, Y.; Petrik, N. G.; Li, Z.; Wang, Z. T.; Glezakou, V. A.; Kay, B. D.; Lyubinetsky, I.; Kimmel, G. A.; Rousseau, R.;

Dohnálek, Z. Structure and Dynamics of CO2 on Rutile TiO2(110) 1 × 1. *J. Phys. Chem. C* **2012**, *116*, 26322–26334.

(63) Cao, Y.; Hu, S.; Yu, M.; Yan, S.; Xu, M. Adsorption and interaction of CO2 on rutile TiO2(110) surfaces: A combined UHV FTIRS and theoretical simulation study. *Phys. Chem. Chem. Phys.* **2015**, *17*, 23994–24000.

(64) Xu, M.; Gao, Y.; Wang, Y.; Wöll, C. Monitoring electronic structure changes of TiO2(110) via sign reversal of adsorbate vibrational bands. *Phys. Chem. Chem. Phys.* **2010**, *12*, 3649–52.

(65) Cao, Y.; Yu, M.; Qi, S.; Ren, Z.; Yan, S.; Hu, S.; Xu, M. Nitric Oxide Reaction Pathways on Rutile TiO2(110): The Influence of Surface Defects and Reconstructions. *J. Phys. Chem. C* **2018**, *122*, 23441–23450.

(66) Xu, M.; Wang, Y.; Hu, S.; Xu, R.; Cao, Y.; Yan, S. NO adsorption and reaction on single crystal rutile TiO2(110) surfaces studied using UHV FTIRS. *Phys. Chem. Chem. Phys.* **2014**, *16*, 14682–14687.

(67) Osmić, M.; Mohrhusen, L.; Al Shamery, K. Bulk Defect Dependence of Low Temperature Partial Oxidation of Methanol and High Temperature Hydrocarbon Formation on Rutile TiO2(110). *J. Phys. Chem. C* **2019**, *123*, 7615–7626.

(68) Mattsson, A.; Hu, S.; Hermansson, K.; Österlund, L. Adsorption of formic acid on rutile TiO2 (110) revisited: An infrared reflection absorption spectroscopy and density functional theory study. *J. Chem. Phys.* **2014**, *140*, 034705.

(69) Mattsson, A.; Hu, S.; Hermansson, K.; Österlund, L. Infrared spectroscopy study of adsorption and photodecomposition of formic acid on reduced and defective rutile TiO2 (110) surfaces. *J. Vac. Sci. Technol., A* **2014**, *32*, 061402.

(70) Mattsson, A.; Osterlund, L. Co adsorption of oxygen and formic acid on rutile TiO2 (110) studied by infrared reflection absorption spectroscopy. *Surf. Sci.* **2017**, *663*, 47–55.

(71) Petrik, N.; Henderson, M.; Kimmel, G. Insights into Acetone Photochemistry on Rutile TiO2 (110). 2. New Photodesorption Channel with CH3 Ejection along the Surface Normal. *J. Phys. Chem. C* **2015**, *119*, 12273–12282.

(72) Kimmel, G. A.; Baer, M.; Petrik, N. G.; VandeVondele, J.; Rousseau, R.; Mundy, C. J. Polarization and Azimuth Resolved Infrared Spectroscopy of Water on TiO2(110): Anisotropy and the Hydrogen Bonding Network. *J. Phys. Chem. Lett.* **2012**, *3*, 778–784.

(73) Petrik, N. G.; Henderson, M. A.; Kimmel, G. A. Insights into Acetone Photochemistry on Rutile TiO2(110). 2. New Photo desorption Channel with CH3 Ejection along the Surface Normal. *J. Phys. Chem. C* **2015**, *119*, 12273–12282.

(74) Petrik, N. G.; Henderson, M. A.; Kimmel, G. A. Insights into Acetone Photochemistry on Rutile TiO2(110). 1. Off Normal CH3 Ejection from Acetone Diolate. *J. Phys. Chem. C* **2015**, *119*, 12262–12272.

(75) Buchholz, M.; Xu, M.; Noei, H.; Weidler, P.; Nefedov, A.; Fink, K.; Wang, Y.; Wöll, C. Interaction of carboxylic acids with rutile TiO2(110): IR investigations of terephthalic and benzoic acid adsorbed on a single crystal substrate. *Surf. Sci.* **2016**, *643*, 117–123.

(76) Clawin, P. M.; Friend, C. M.; Al Shamery, K. Defects in surface chemistry Reductive coupling of benzaldehyde on Rutile TiO2(110). *Chem. Eur. J.* **2014**, *20*, 7665–7669.

(77) Setvin, M.; Buchholz, M.; Hou, W.; Zhang, C.; Stöger, B.; Hulva, J.; Simschitz, T.; Shi, X.; Pavelec, J.; Parkinson, G. S.; Xu, M.; Wang, Y.; Schmid, M.; Wöll, C.; Selloni, A.; Diebold, U. A Multitechnique Study of CO Adsorption on the TiO2 Anatase (101) Surface. *J. Phys. Chem. C* **2015**, *119*, 21044–21052.

(78) Xu, M.; Noei, H.; Buchholz, M.; Muhler, M.; Wöll, C.; Wang, Y. Dissociation of formic acid on anatase TiO2(101) probed by vibrational spectroscopy. *Catal. Today* **2012**, *182*, 12–15.

(79) Schöttner, L.; Nefedov, A.; Yang, C.; Heissler, S.; Wang, Y.; Wöll, C. Structural Evolution of α Fe2O3(0001) Surfaces Under Reduction Conditions Monitored by Infrared Spectroscopy. *Front. Chem.* **2019**, *7*, 1–12.

(80) Schöttner, L.; Ovcharenko, R.; Nefedov, A.; Voloshina, E.; Wang, Y.; Sauer, J.; Wöll, C. Interaction of Water Molecules with the

α Fe2O3(0001) Surface: A Combined Experimental and Computational Study. *J. Phys. Chem. C* **2019**, *123*, 8324−8335.

(81) Gamba, O.; Noei, H.; Pavelec, J.; Bliem, R.; Schmid, M.; Diebold, U.; Stierle, A.; Parkinson, G. S. Adsorption of Formic Acid on the Fe3O4(001) Surface. *J. Phys. Chem. C* **2015**, *119*, 20459−20465.

(82) Yang, C.; Bebensee, F.; Nefedov, A.; Wöll, C.; Kropp, T.; Komissarov, L.; Penschke, C.; Moerer, R.; Paier, J.; Sauer, J. Methanol adsorption on monocrystalline ceria surfaces. *J. Catal.* **2016**, *336*, 116−125.

(83) Yang, C.; Yu, X.; Pleßow, P.; Heissler, S.; Weidler, P.; Nefedov, A.; Studt, F.; Wang, Y.; Wöll, C. Rendering Photoreactivity to Ceria: The Role of Defects. *Angew. Chem., Int. Ed.* **2017**, *56*, 14301−14305.